RESEARCH ARTICLE SUMMARY

COASTAL DYNAMICS

Unexpected expansion and regrowth in Earth's mangrove forests over the past four decades

Zhen Zhang*, Nicholas J. Murray, Xiao-Peng Song, Pete Bunting, Thomas A. Worthington, Lola Fatoyinbo, Dehua Mao, Mingming Jia, Virni Budi Arifanti, Toh Aung, San San Htay, Daniel A. Friess*

Full article and list of author affiliations: https://doi.org/10.1126/science.aec9773

INTRODUCTION: Mangrove forests are globally important coastal ecosystems, playing a disproportionate role in climate regulation, coastal protection, and the maintenance of biodiversity. Despite their importance, it is generally acknowledged that mangroves have declined rapidly over recent decades as a result of deforestation and shoreline erosion; and they are widely considered one of the most threatened ecosystems globally. In the face of increasing pressures from anthropogenic activities and climate change, understanding mangrove dynamics is critical for quantifying changes in the ecosystem services they provide and for informing global conservation and restoration targets.

RATIONALE: Mangrove forests can partially recover lost area through natural regeneration and can also expand by colonizing newly formed tidal flats. In addition to changes in areal extent, mangrove stands can undergo substantial canopy thinning or accumulation without experiencing outright loss or gain. It remains unclear to what extent mangrove regeneration and expansion have offset historical losses globally, and subtle but widespread variations in canopy condition within persistent mangroves remain largely unquantified. To address these gaps, we developed an annual global dataset of mangrove extent and canopy cover spanning the past four decades using long-term Landsat observations. This framework enables a unified assessment of both binary area change (loss and gain) and continuous canopy dynamics within persistent mangrove forests, including degradation (canopy thinning) and growth (canopy accumulation).

RESULTS: Global mangrove loss rates reduced substantially from the 1980s to 2023, while mangrove gains increased markedly over the same period. As a result, global mangrove extent shifted from net loss to near gain in the recent decade, driven primarily by natural seaward expansion. This recent increase in gains has offset a large fraction of historical losses, resulting in only a marginal net loss in global mangrove area since the 1980s. Beyond areal change, we detected widespread mangrove degradation, which was more extensive than loss and was strongly associated with tropical cyclones, although degradation rates also declined over time. Meanwhile, persistent mangrove forests continued to accumulate canopy cover through natural growth, leading to an expansion of dense-canopy mangroves.

CONCLUSION: Our findings demonstrate that even highly disturbed ecosystems such as mangroves retain a strong resilience for recovering from loss or degradation. By highlighting the dominant role of natural expansion and regeneration, our results suggest that halting deforestation should be prioritized to meet current global mangrove area targets. Furthermore, those newly established mangroves represent an important opportunity for conservation, because young stands require time to accumulate carbon and fully recover the ecosystem functions of the mangroves that they replaced. Understanding the mechanisms governing mangrove expansion and regeneration is therefore essential for guiding effective mangrove restoration. □

*Corresponding author. Email: zzhang58@tulane.edu (Z.Z.); dfriess@tulane.edu (D.A.F.)
Cite this article as Z. Zhang *et al.*, *Science* **392**, 1082 (2026). DOI: 10.1126/science.aec9773

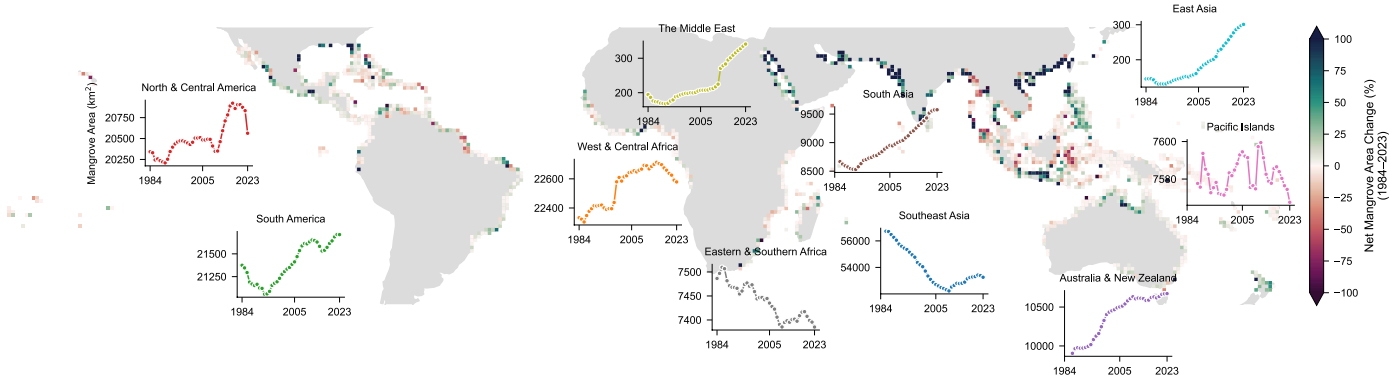

Global patterns and regional trajectories of mangrove area change (1984–2023). Colors indicate net percentage change in mangrove area at the 1° grid cell scale. Insets show regional mangrove area trajectories at annual frequency.

COASTAL DYNAMICS

Unexpected expansion and regrowth in Earth's mangrove forests over the past four decades

Zhen Zhang[1]*, Nicholas J. Murray[2], Xiao-Peng Song[3], Pete Bunting[4], Thomas A. Worthington[5], Lola Fatoyinbo[6,7], Dehua Mao[8], Mingming Jia[8], Virni Budi Arifanti[9], Toh Aung[10], San San Htay[11], Daniel A. Friess[1]*

Global mangrove forests have disappeared rapidly because of deforestation but have also regrown through natural regeneration and restoration. Yet their long-term trends in extent and canopy cover remain poorly quantified. By developing a global dataset of annual mangrove extent and canopy cover, we show that losses (long-term conversion) and degradation (canopy thinning) have both reduced since the 1980s and have been largely offset by regeneration and seaward expansion in the past decade. Consequently, global mangrove extent has shifted from net loss to net gain since around 2010 and changed only marginally from the 1980s to 2023 (−0.5% ± 1.4%). Beyond changes in extent, persistent mangroves exhibited sustained canopy accumulation. Our findings reveal the underestimated resilience of a highly threatened ecosystem, demonstrate early conservation effectiveness, and highlight halting deforestation as a priority for achieving conservation targets through natural regrowth.

Mangrove forests are an important component of the global carbon cycle owing to their exceptionally high carbon density and long-term carbon storage (*1*), making their conservation a promising natural solution for climate change mitigation (*2*, *3*). Changes in mangrove extent and condition directly affect the delivery of their diverse services to people (*4*) and have important implications for the sustainability and resilience of the land-sea interface (*5*, *6*). However, expansion of aquaculture, agriculture, and urban development has driven substantial mangrove loss since the 19th century, peaking in the 20th century (*7*). Natural disturbances, such as shoreline erosion, also pose serious threats to mangrove forests (*8*). Consequently, global assessments have consistently concluded that mangroves remain in persistent decline (*9*, *10*).

To halt and reverse this trend, many countries have launched ambitious mangrove restoration initiatives, such as Indonesia's National Mangrove Management Strategy (*11*) and China's Special Action Plan for Mangrove Conservation and Restoration, which has already shown early signs of bringing about recovery (*12*, *13*). Mangroves also have an inherent capacity to colonize newly available habitats (*14*) and regenerate under favorable conditions (*15*), such as within abandoned aquaculture ponds (*16*). However, the extent to which the combined processes of natural expansion, natural regeneration, and human-assisted restoration have offset historical mangrove losses remains poorly understood.

Even in the absence of complete loss, mangrove canopy cover can still experience damage resulting from either natural disturbances [e.g., cyclones (*17*) and climatic oscillations (*18*)] or anthropogenic impacts (e.g., selective logging), a process often referred to as degradation (*7*, *19*). Such within-mangrove change has a range of ecological consequences, including carbon emissions, reduced coastal protection, and loss of biodiversity (*20*). Mangroves are also known for their resilience to disturbance and can recover rapidly, for example, returning to precyclone leaf area within just 1 year (*21*). Yet little is known about the global rates and spatial extent of mangrove degradation and growth, the processes representing within-mangrove canopy changes without complete loss or gain, which hinders our understanding of the full spectrum of mangrove dynamics and their impacts on carbon storage and ecosystem services.

In this study, we quantified global mangrove canopy dynamics by developing a high-resolution (30 m) annual product of mangrove extent and fractional canopy cover (FCC) from 1984 to 2023 (fig. S1). Annual mangrove extents were categorized into four canopy conditions: closed mangrove forests (FCC >80%), open mangrove forests (50 to 80%), mangrove woodland (20 to 50%), and sparse mangroves (<20%) (*22*) (fig. S2). Four types of mangrove dynamics were then distinguished (fig. S3): (i) loss, defined as complete conversion of mangroves to other land covers for at least 3 years, whether driven by natural or anthropogenic factors (deforestation); (ii) gain, defined as new mangroves gained in locations where mangrove forests had been lost (regeneration) or from areas that were not previously mangrove within our time series (expansion) (fig. S4A); (iii) degradation, defined as a shift to a lower-cover category accompanied by a minimum FCC decline of 20% within persistent mangroves (*23*), or as a short-term loss of mangroves (<3 years) (fig. S4B) (*24*); and (iv) growth, defined as a substantial increase in FCC of persistent mangrove areas (*25*, *26*) (the opposite of degradation). By distinguishing between mangrove land-cover transitions and within-mangrove canopy changes, we provide a clear and consistent picture of their global extent and long-term trajectory, offering new insights into global mangrove dynamics.

A shift from net loss to net gain

Four decades of satellite monitoring reveal a reversal in the global trajectory of mangrove extent. Between the 1980s and 2010, global mangrove extent declined from 154,810 km^2 [95% confidence interval (CI): 140,661 to 158,069 km^2] to 151,928 km^2 (139,539 to 154,633 km^2, 95% CI), representing a net loss of 2882 km^2 (1.86%, 95% CI: −4939 to −1025 km^2). However, this trend reversed in the subsequent decade. By 2023, global mangrove area had rebounded to 153,961 km^2 (145,085 to 158,206 km^2, 95% CI), reflecting a net gain of 2033 km^2 (1.34%, 95% CI: 1131 to 3158 km^2) since 2010 and resulting in a marginal net loss of just 849 km^2 (95% CI: −2927 to 1360 km^2) over the entire 1980s-to-2023 period (table S1). This small net loss underscores the substantial compensatory effect of mangrove gains. Between the 1980s and 2010, 12,657 km^2 or 8.2% (−14,317 to −10,283 km^2, 95% CI) of mangroves were lost, yet 9775 km^2 (7467 to 11,566 km^2, 95% CI) of new mangrove forests were established, mitigating 77% of gross losses. Mangrove gain accelerated from a pre-2010 average of 0.28% per year to 0.42% per year during 2010–2023, contributing 8307 km^2 (6660 to 9492 km^2, 95% CI) of new mangroves that outpaced 6275 km^2 (−7696 to −4539 km^2, 95% CI) of loss (table S1).

The observed widespread mangrove gains contrast with earlier global assessments (*9*, *10*), which reported persistent declines (fig. S5). Our analysis detected substantially more mangrove changes, particularly gains, than the widely used Global Mangrove Watch (GMW) v3.0

[1]Department of Earth and Environmental Sciences, Tulane University, New Orleans, LA, USA. [2]College of Science and Engineering, James Cook University, Townsville, Australia. [3]Department of Geographical Sciences, University of Maryland, College Park, MD, USA. [4]Department of Geography and Earth Sciences, Aberystwyth University, Aberystwyth, Wales, UK. [5]Department of Plant Sciences, University of Cambridge, Cambridge, UK. [6]Space Enabled Research Group, Department of Media Arts and Sciences, Massachusetts Institute of Technology, Cambridge, MA, USA. [7]Biospheric Sciences Laboratory, National Aeronautics and Space Administration (NASA) Goddard Space Flight Center, Greenbelt, MD, USA. [8]Key Laboratory of Wetland Ecology and Environment, Northeast Institute of Geography and Agroecology, Chinese Academy of Sciences, Changchun, China. [9]Research Center for Ecology, National Research and Innovation Agency of the Republic of Indonesia, Cibinong, Indonesia. [10]Natural Resources Governance and Environment, Yangon, Myanmar. [11]Climate Change and Blue Carbon Program, Yangon, Myanmar.
***Corresponding author. Email: zzhang58@tulane.edu (Z.Z.); dfriess@tulane.edu (D.A.F.)**

product (*10*) (fig. S6). These differences likely arise from the underlying data sources: Our workflow uses optical imagery, which is highly sensitive to canopy reflectance, whereas GMW v3.0 relies on radar backscatter, which is less responsive to early-stage mangrove gain, owing to subtle changes in radar signals. Moreover, the continuous Landsat record provides globally consistent long-term observations, whereas GMW v3.0 integrates multiple radar sensors, introducing misregistration and additional uncertainty in change detection. For example, the 1996 JERS-1 imagery used by GMW v3.0 uses horizontal-horizontal polarization, which is inherently less sensitive to mangrove canopy structure than the horizontal-vertical polarization used in later years, leaving the baseline mangrove layer with greater uncertainty.

Separating global signals by biogeographic region (fig. S7A) reveals that net mangrove loss from the 1980s to 2010 was overwhelmingly concentrated in Southeast Asia (table S1), which accounted for 59.3% of global mangrove losses, followed by the Americas (22.5%). Key hotspots included Kalimantan, Sulawesi, Sumatra, Myanmar, the Caribbean, and parts of Brazil (Fig. 1). Notably, the rate of net loss in Southeast Asia peaked between 1990 and 2005 but has since slowed, with the region transitioning to net gain after 2010 (Fig. 2A). This shift reflects the combined effects of post-2005 stabilization in Indonesia and post-2010 gains in Myanmar (figs. S8 and S9). In Indonesia, rapid loss between 1995 and 2005 was followed by stabilization, likely associated with increased awareness and restoration after the 2004 Indian Ocean tsunami (*11*), and strengthened legal protection and management since the early 2000s (*27*). In Myanmar, mangrove area transitioned from consistent decline to net gain after 2010, particularly in the Irrawaddy delta, Gulf of Martaban, and the Naf River region along the Myanmar-Bangladesh border (fig. S10). This reversal in Myanmar is robust across two independent mapping approaches (fig. S10B) and can be explained by reduced mangrove disturbances after 2010 (*28*), natural expansion on mudbanks (*29*, *30*), increased awareness after the devastating impact of Cyclone Nargis in 2008 (*31*), a national mangrove logging ban passed in 2014 (*32*), and active plantation and restoration efforts (*33*). Despite a 10% increase in mangrove area since 2010, Myanmar experienced a net loss of 28.6% between the 1980s and 2010, remaining the most severely mangrove-deforested major country (Fig. 2B). By contrast, West and Central Africa show the opposite trend. After decades of expansion, particularly in Senegal, Gambia, and Guinea-Bissau, the region shifted to net loss around 2014, driven largely by accelerating losses in Nigeria since 2002 (fig. S8).

Outside of Southeast Asia and Africa, all remaining regions exhibited long-term net gains in mangrove areas (Fig. 2A), which were particularly pronounced in northern Australia, western Mexico, the Gulf of Mexico, the Middle East, and South Asia (Fig. 1). Specifically, in Australia and New Zealand, mangrove gains were most rapid between 1987 and 2010 (Fig. 2A); South Asia, East Asia, and the Middle East each demonstrated near-linear increases in mangrove extent since the 1990s (Fig. 2A). These findings are consistent with

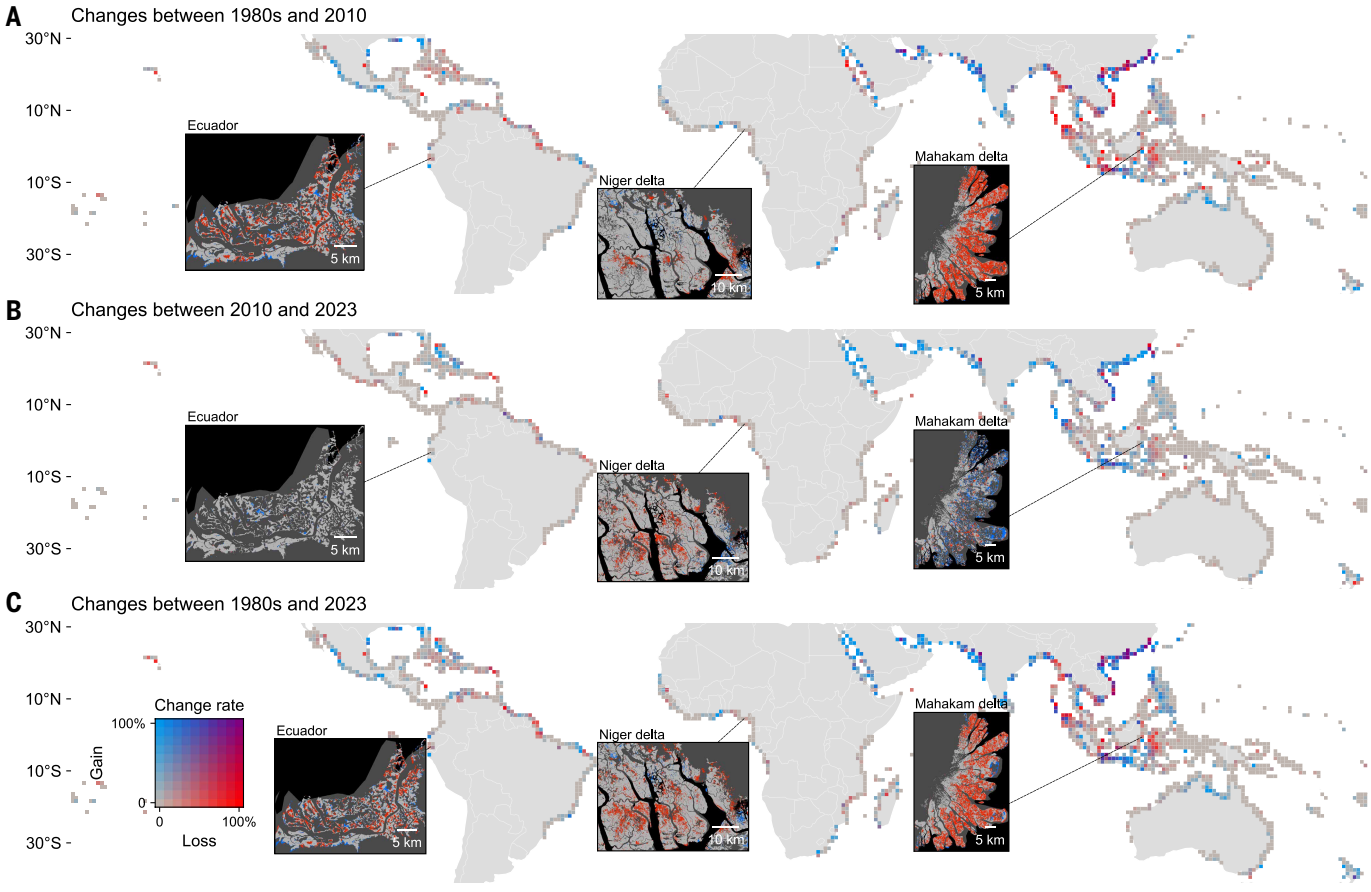

Fig. 1. Global pattern of mangrove loss and gain from the 1980s to 2023. Mangrove changes are shown for (**A**) the 1980s to 2010, (**B**) 2010 to 2023, and (**C**) the 1980s to 2023. The 1980s map represents a baseline mangrove extent map derived from the earliest available Landsat observations for each pixel. The color scale, shown on the bottom left, indicates the rate of change in terms of both loss (red) and gain (blue), with 0% change represented by gray. The rate is calculated as (Δarea/original area) × 100%. Inset regional maps provide detailed examples of change patterns for Ecuador, the Niger delta of Nigeria, and the Mahakam delta of Indonesia, where blue patches indicate mangrove gain, red patches signify loss, and gray patches indicate persistent mangrove areas.

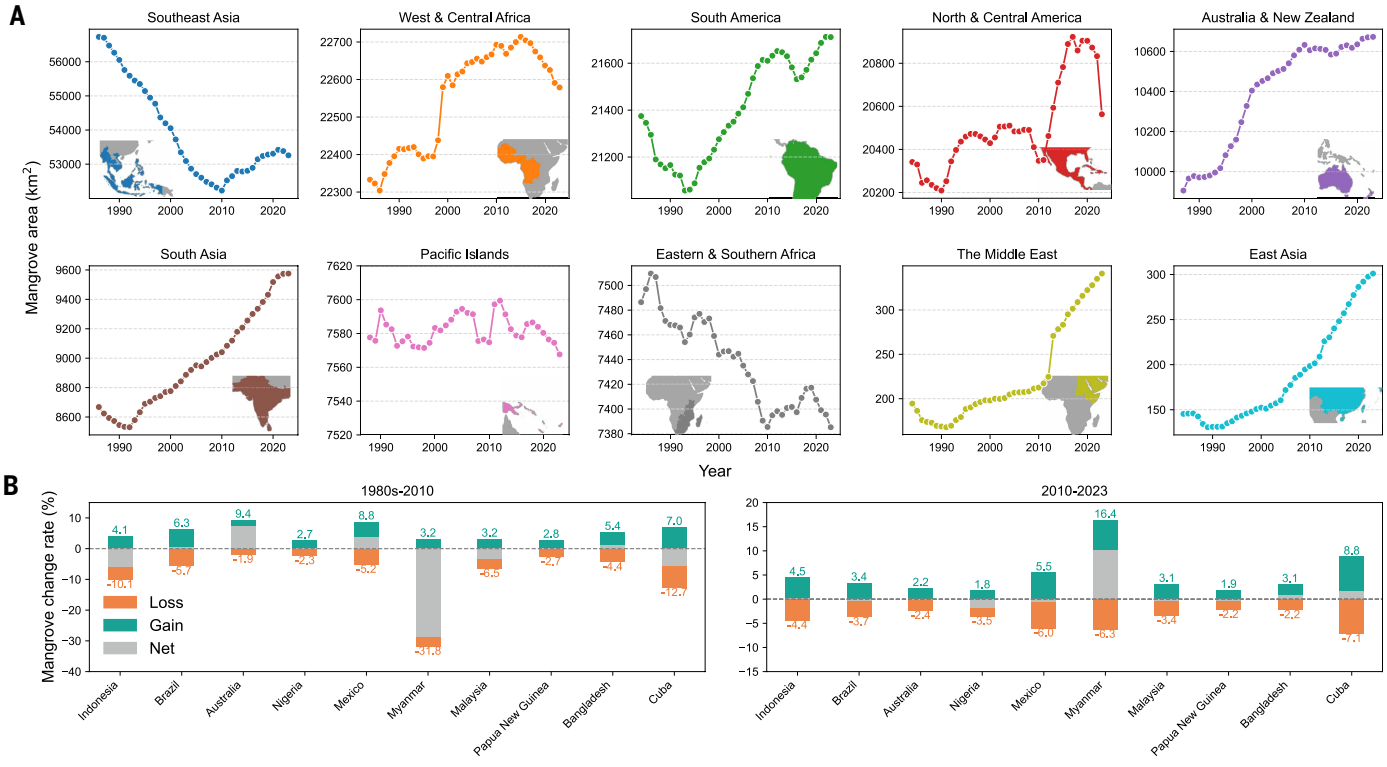

Fig. 2. Regional mangrove area dynamics and country-level change rates. (**A**) Time series of mangrove areas (km^2) from the 1980s to 2023 for each biogeographical region. Within each plot, the inset map shows the corresponding geographical extent. (**B**) Mangrove change rates for the top 10 mangrove-rich nations, ordered by their mangrove extent. Teal bars indicate gain rates, orange bars show loss rates, and gray bars represent the net change rate. Note that (A) presents map-based annual area estimates only; formal confidence intervals cannot be provided at annual and regional scales without extensive region-specific accuracy assessments.

regional observations documenting net mangrove gains in Australia (*22*), East Asia (*12*), Senegal (*34*), Brazil (*35*), and the Middle East (*36*).

Mangrove gains after 2010 were dominated by expansion rather than regeneration. Of the 7476 km^2 of global gains from 2010 to 2023, expansion accounted for 5364 km^2 (64.6%), with regeneration comprising the remaining 35.4% (fig. S11). Expansion usually occurred in deltaic and riverine areas (fig. S11, C to F), which is consistent with natural colonization processes. A striking hotspot of mangrove expansion is the northeastern coastline of South America, where mudbanks formed by Amazon River sediment provide new habitats for rapid mangrove colonization (*37*). This reflects the ecological adaptability of mangroves to colonize bare mudflats when environmental conditions are within their physiological tolerance (*38*). Observed mangrove gains also align with reported net area gains in global deltas due to increased sediment input from upstream deforestation and mining (*39*–*41*), reflecting that the rate of mangrove gain in minerogenic settings is highly dependent on terrigenous sediment supply.

Mangrove degradation and loss are slowing down

Distinguishing between mangrove loss and degradation is critical because they could be driven by different processes, have distinct ecological consequences, and require tailored conservation strategies (*7*). Our long-term record of canopy cover reveals that mangrove degradation affects a much larger area than loss. On average, annual degradation rates exceeded loss rates across 64.9% of global mangrove area, being particularly evident in Africa, the Caribbean, and the Pacific Islands (Fig. 3A). Southeast Asia exhibited high rates of both degradation and loss, especially in mainland regions. In certain years, degradation was several-fold higher than loss, such as in South Asia (2008), Eastern and Southern Africa (2000), North and Central America (2017), and Australia and New Zealand (2011) (Fig. 3B). These abrupt degradation events coincided closely with the passage of tropical cyclones (fig. S12), such as Cyclone Yasi in Australia (2011), Hurricane Irma in Cuba and Florida , USA (2017), Cyclone Rashmi in the Sundarbans (2008), and Cyclone Leon-Eline in Mozambique (2000), confirming tropical cyclones as a dominant driver of mangrove degradation globally. Human activities have also played an important role in mangrove degradation. For example, crude oil pollution has caused extensive and long-term damage to mangrove ecosystems in the Niger delta (*42*).

Mangrove disturbance (degradation and loss) rates have declined over the past four decades, mostly because of reductions in degradation, which fell from ~0.64% $year^{-1}$ in the 1980s to 0.24% $year^{-1}$ by the recent decade (fig. S13). The average loss rate of mangroves during the recent decade was also around 0.24% $year^{-1}$, comparable to 1985–1995 but lower than 1995–2005 (0.33% $year^{-1}$), suggesting a reduction in mangrove loss rate since around 2000. Southeast Asia exhibited substantial decreases in annual rates of both mangrove degradation and loss, with loss rates rising between 1988 and 1998, subsequently declining until 2011, and stabilizing thereafter at around 0.29% $year^{-1}$ (Fig. 3B). These patterns are consistent with previous findings (*43*–*45*) and reflect the cumulative impact of conservation efforts (*46*), reduced tropical cyclone frequency in some regions (*47*), and increased agroforestry practices (*48*). However, these declines in disturbance were partly offset by rising rates in West and Central Africa, which has emerged as the current hotspot of mangrove degradation, reaching ~0.53% $year^{-1}$ during 2015–2023, primarily concentrated in the Niger delta (fig. S14). These nonlinear dynamics underscore the importance of tracking fine-scale temporal variation in mangrove disturbance.

Despite an overall reduction, mangrove disturbance still persists in recent years (2018–2023) (fig. S15). Some of these events were associated with climatic extremes, such as mangrove dieback in Texas, USA, after a severe freeze in 2021; damage from Hurricane Ian in Florida, USA, and Cuba (2022); and canopy loss in Mexico's Marismas Nacionales-San Blas

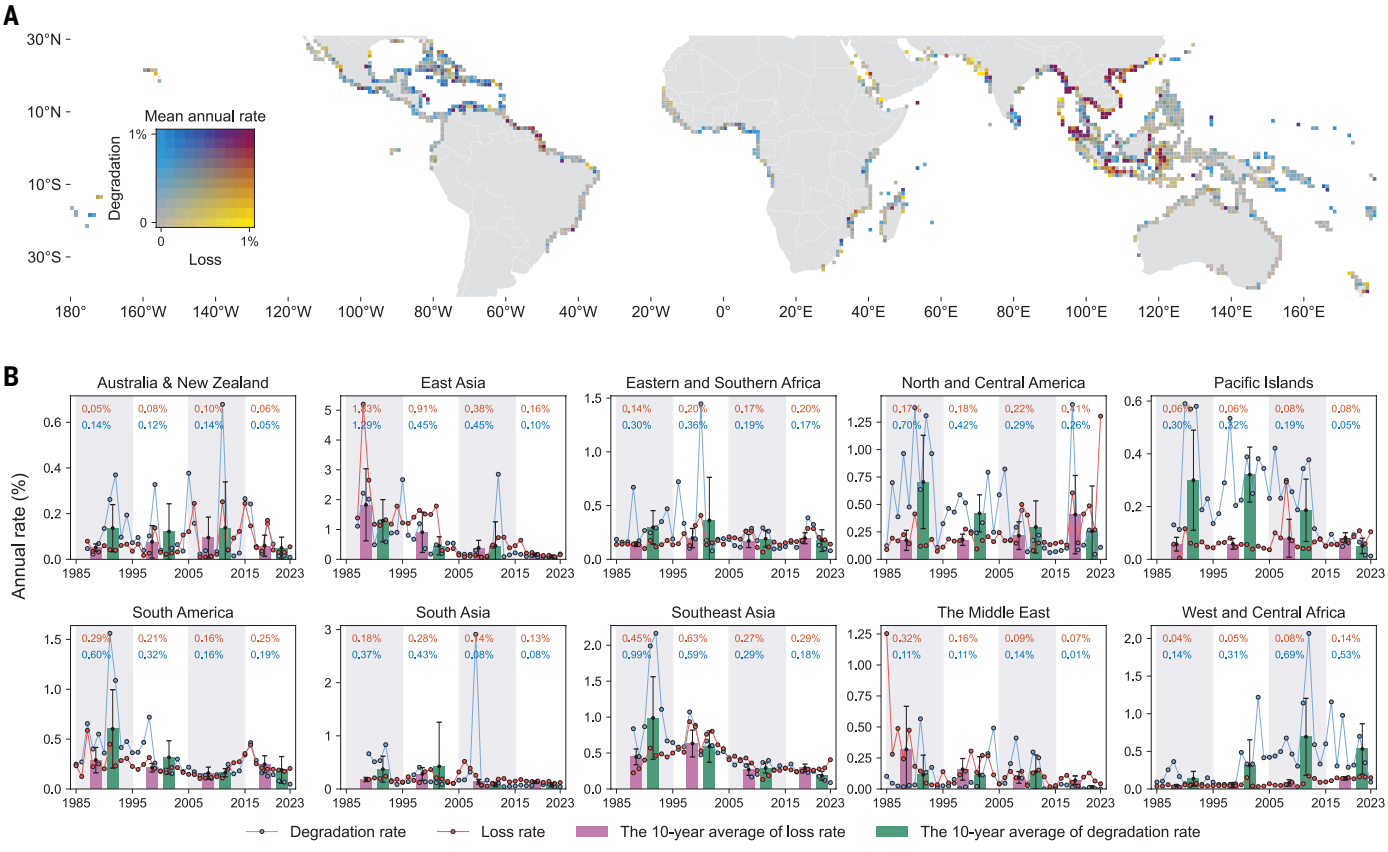

Fig. 3. Global and regional rates of mangrove disturbance consisting of loss and degradation. (**A**) Global pattern of long-term average annual disturbance rates. The color key indicates the mean annual rate, with increasing degradation toward blue and increasing loss toward yellow, with dark magenta representing high rates of both and gray representing low rates for both. (**B**) Temporal profiles of annual rates for 10 biogeographical regions. Individual points and thin lines show the annual rates of loss (red) and degradation (blue). Temporal peaks in disturbance rates align closely with tropical cyclone events, such as Cyclone Rashmi in 2008 in South Asia (fig. S12). The bars represent the 10-year average rate of loss (pink) and degradation (green), with error bars indicating the corresponding 10-year standard deviation. Numbers within each regional panel correspond to the 10-year average rate for loss (red) and degradation (blue).

mangrove ecoregion after Hurricane Roslyn (2022) (fig. S16). Shoreline erosion still contributes to mangrove loss, such as along the Amazon-Guianas Atlantic coastline (fig. S16C). Anthropogenic deforestation also remains widespread, even within formally protected areas. A striking example is the Rufiji delta in Tanzania, which is a Ramsar-designated protected area but is experiencing excessive mangrove deforestation due to conversion to rice farms (*49*) (fig. S16E).

Increased canopy cover of mangrove forests

Although abrupt mangrove degradation events have occurred in specific years, a broader decadal perspective reveals a net gain in canopy cover, as evidenced by an increase in the extent of closed-canopy mangrove forests (FCC >80%). Globally, closed mangrove forests increased from 77,643 km^2 (50.2% of total mangrove area) in the 1980s to 88,772 km^2 (57.7% of total) by 2023, even though total mangrove area has slightly decreased. Increases in closed mangrove forests from the 1980s to 2023 were high in South America [31.2% (3548 km^2) of total increases], mostly taking place along the Amazon Macrotidal Mangrove Coast (Fig. 4, A and B). Closed mangrove forests in the Middle East, western South Asia, and East Asia experienced large increases in terms of proportion (fig. S17), probably due to range expansion (*50*) and restoration efforts (*51*). Eastern and Central Africa is the only biogeographic region with decreased closed mangrove forests, which are concentrated mostly in Madagascar (Fig. 4A).

Closed mangrove forests are preferentially targeted for deforestation. Between the 1980s and 2023, closed mangroves accounted for nearly half of global gross mangrove loss (48.6%, −6866 km^2), two-thirds of which (66.7%, −4581 km^2) occurred in Southeast Asia. Despite these losses, the total area of closed mangroves still increased, primarily driven by canopy growth within persistent mangroves, particularly transitions from open- to closed-canopy conditions (Fig. 4D). Such canopy growth offset losses of closed mangroves in Southeast Asia, resulting in a largely stable extent of closed-canopy mangroves. These findings demonstrate that, in the absence of loss, mangrove forests have a strong capacity to accumulate canopy cover, which could contribute to increased primary productivity (*52*).

Another contributor to the net increase in closed mangrove forests is from newly established forests. Of mangroves that developed since the 1980s, 42.8% (5679 km^2) had reached closed-canopy condition by 2023. Even among younger mangroves established after 2010, 33.5% (2783 km^2) transitioned to closed-canopy conditions, with expansion slightly more likely to achieve closure (34.8%) than regeneration (31.2%). These results indicate that the formation of closed mangrove forests can occur rapidly. As of 2023, 42.3% of global mangrove forests remain in open or woodland states, representing a substantial potential reservoir for future development of closed-canopy forests under effective protection.

The expansion of closed-canopy forests could enhance sediment trapping, promoting adaptation to sea-level rise and supporting lateral expansion (*53*), thus suggesting a positive-feedback mechanism in mangrove development. Moreover, increases in canopy cover without associated land-cover change imply net accumulation of biomass and carbon storage. These findings indicate that assessments of blue carbon

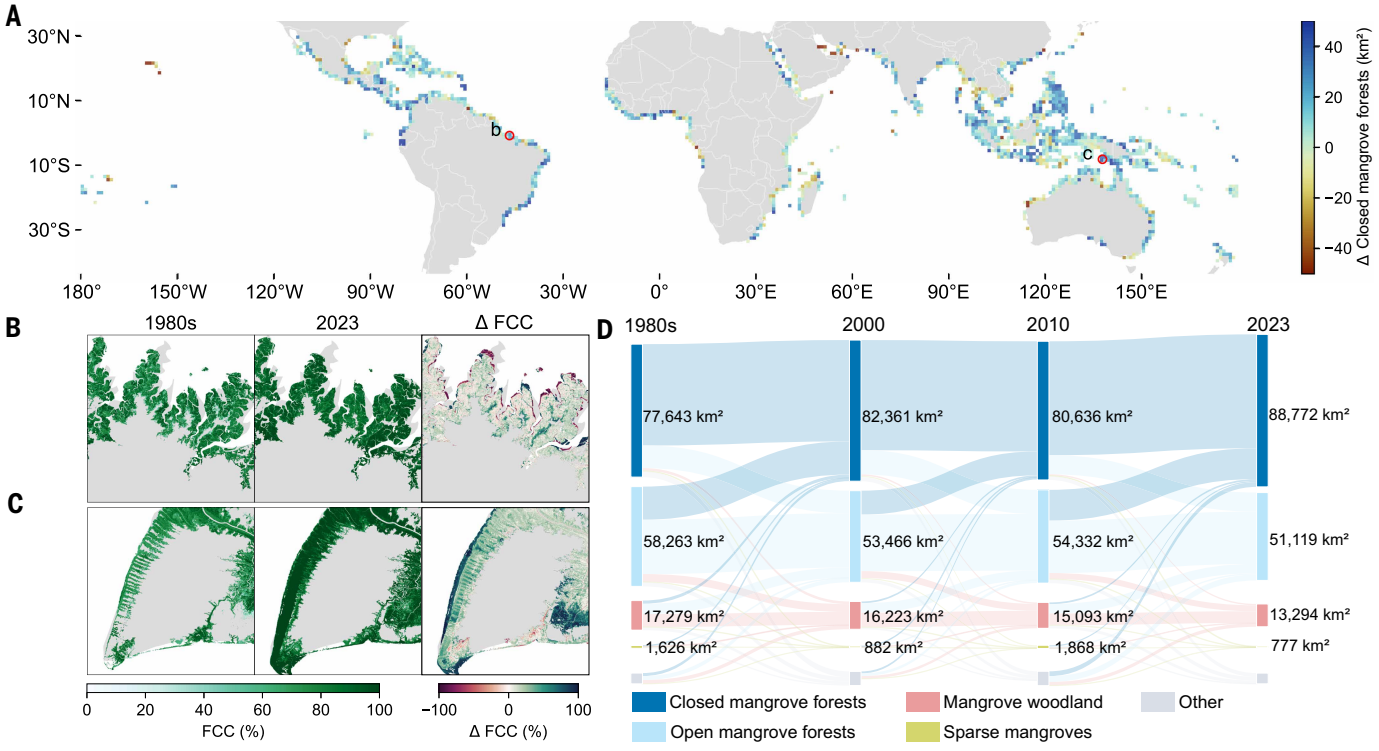

Fig. 4. Dynamics of mangrove canopy cover. (**A**) Global pattern of area change (km^2) of closed mangrove forests from the 1980s to 2023. The color map indicates the magnitude of change, with blue representing increases and brown representing decreases in area. The two red circles highlight the locations of the regional examples detailed in (B) and (C) (Amazon Macrotidal Mangrove Coast and southwestern Papua, respectively). (**B** and **C**) Regional examples illustrating mangrove change. For each region, the left and middle subpanels display FCC images from the 1980s composite baseline map and 2023, respectively, where darker green indicates higher canopy cover. The right subpanels show the change in FCC (ΔFCC = 2023 FCC − 1980s FCC), with greener areas indicating increased FCC (i.e., mangrove growth). (**D**) Sankey diagram illustrating the flow and area (km^2) of different mangrove canopy types across four time points: 1980s, 2000, 2010, and 2023, which highlights the overall increase in closed mangrove forest area, primarily transferred from open mangrove forests.

dynamics based solely on areal extent (*5*) may underestimate carbon emission and uptake, particularly where structural canopy changes are not accounted for. However, newly formed closed-canopy mangrove stands are not necessarily equivalent to mature forests in ecosystem function, with younger stands providing reduced ecological services relative to older, deforested mangroves (*54*). As such, offsetting functional losses from deforestation through mangrove gain requires not only spatial compensation but also sufficient time for ecosystem maturation and full functional recovery.

Conclusions

Our results reveal widespread global mangrove expansion and regrowth, resulting in a net gain of mangroves in the recent decade. Although part of this increase may reflect ongoing restoration efforts, the large magnitude and seaward expansion patterns suggest that it is more likely driven by the intrinsic capacity of mangroves for colonization of new intertidal habitats and natural regeneration of areas that were previously mangroves. This indicates that even highly threatened ecosystems, such as mangroves exposed to both anthropogenic disturbance and climate change, can exhibit greater resilience to maintain their area than previously recognized. However, the ability for mangroves to expand in area should not be interpreted as grounds for complacency. Instead, it highlights the substantial potential to harness natural recovery and colonization processes in mangrove conservation. Current conservation efforts often emphasize mangrove planting and area-based targets (*55*) but may overlook the substantial contribution of natural gain and increased canopy growth. Conservation strategies could therefore prioritize halting deforestation, while enabling natural expansion and regeneration once biophysical and human pressures are reduced. Additionally, conservation frameworks must look beyond area-based targets alone. Gains in canopy cover, such as transitions from open to closed mangrove forests, can also enhance ecological functioning such as carbon uptake. Newly established mangroves warrant particular attention because understanding the processes underlying their expansion is critical for guiding restoration and maximizing carbon sequestration. These young forests also represent a substantial and growing carbon sink (*56*), but because of underdeveloped trunks and anchoring root systems, they may be more vulnerable to disturbances such as cyclones. Conservation policies, therefore, could place emphasis on protecting naturally generated mangroves rather than relying predominantly on planting. Our findings offer a new basis for understanding and predicting mangrove dynamics, advancing global ecosystem restoration goals, and refining strategies for climate change mitigation through blue carbon ecosystems.

REFERENCES AND NOTES

1. D. C. Donato *et al.*, *Nat. Geosci.* **4**, 293–297 (2011).
2. D. Murdiyarso *et al.*, *Nat. Clim. Chang.* **5**, 1089–1092 (2015).
3. P. I. Macreadie *et al.*, *Nat. Rev. Earth Environ.* **2**, 826–839 (2021).
4. S. Y. Lee *et al.*, *Glob. Ecol. Biogeogr.* **23**, 726–743 (2014).
5. S. E. Hamilton, D. A. Friess, *Nat. Clim. Chang.* **8**, 240–244 (2018).
6. T. Tiggeloven *et al.*, *Proc. Natl. Acad. Sci. U.S.A.* **123**, e2510980123 (2026).
7. D. A. Friess *et al.*, *Annu. Rev. Environ. Resour.* **44**, 89–115 (2019).
8. Y. Xiong *et al.*, *Commun. Earth Environ.* **7**, 417 (2026).
9. N. J. Murray *et al.*, *Science* **376**, 744–749 (2022).
10. P. Bunting *et al.*, *Remote Sens.* **14**, 3657 (2022).
11. S. D. Sasmito *et al.*, *Nat. Ecol. Evol.* **7**, 62–70 (2023).

12. X. Wang *et al.*, *Nat. Sustain.* **4**, 1076–1083 (2021).
13. X. Ouyang, F. Guo, S. Y. Lee, Z. Yang, *Science* **385**, 836–836 (2024).
14. N. Panapitukkul *et al.*, *Estuar. Coast. Shelf Sci.* **47**, 51–61 (1998).
15. V. Otero *et al.*, *For. Ecol. Manage.* **472**, 118213 (2020).
16. Y. Jiang *et al.*, *One Earth* **8**, 101149 (2025).
17. J. Peereman, J. A. Hogan, T.-C. Lin, *Glob. Ecol. Biogeogr.* **31**, 37–50 (2022).
18. Z. Zhang, X. Luo, D. A. Friess, Y. Li, *Nat. Geosci.* **18**, 488–494 (2025).
19. E. S. Yando *et al.*, *Biol. Conserv.* **263**, 109355 (2021).
20. L. Carugati *et al.*, *Sci. Rep.* **8**, 13298 (2018).
21. D. Reed *et al.*, *Glob. Change Biol.* **31**, e70124 (2025).
22. L. Lymburner *et al.*, *Remote Sens. Environ.* **238**, 111185 (2020).
23. S. Wei, H. Zhang, J. Ling, *GIsci. Remote Sens.* **62**, 2491920 (2025).
24. C. Vancutsem *et al.*, *Sci. Adv.* **7**, eabe1603 (2021).
25. Y. Liu *et al.*, *Sci. Data* **11**, 832 (2024).
26. T. T. Caughlin, S. W. Rifai, S. J. Graves, G. P. Asner, S. A. Bohlman, *Remote Sens. Ecol. Conserv.* **2**, 190–203 (2016).
27. V. B. Arifanti *et al.*, *Forests* **13**, 695 (2022).
28. Y. Xia, K. Liu, Y. Zhu, X. Wen, J. Cao, *Environ. Monit. Assess.* **197**, 762 (2025).
29. P. P. Thant *et al.*, *Mar. Environ. Res.* **210**, 107343 (2025).
30. K. Win, J. Sasaki, *Remote Sens.* **16**, 4077 (2024).
31. T. T. Aung, Y. Mochida, M. M. Than, *For. Ecol. Manage.* **293**, 103–113 (2013).
32. G. W. Prescott *et al.*, *Conserv. Biol.* **31**, 1257–1270 (2017).
33. W. M. Aye, S. Takeda, *Paddy Water Environ.* **18**, 417–429 (2020).
34. J. Andrieu *et al.*, *For. Ecol. Manage.* **461**, 117963 (2020).
35. G. T. Vanin, E. R. Lacerda, G. M. Mori, *Conserv. Biol.* **39**, e14426 (2025).
36. H. Almahasheer, A. Aljowair, C. M. Duarte, X. Irigoien, *Estuar. Coast. Shelf Sci.* **169**, 164–172 (2016).
37. E. J. Anthony *et al.*, *Earth Sci. Rev.* **103**, 99–121 (2010).
38. C. Proisy *et al.*, *Cont. Shelf Res.* **29**, 632–641 (2009).
39. J. H. Nienhuis *et al.*, *Nature* **577**, 514–518 (2020).
40. E. N. Dethier *et al.*, *Nature* **620**, 787–793 (2023).
41. X. Hou, D. Xie, L. Feng, F. Shen, J. H. Nienhuis, *Nat. Commun.* **15**, 3319 (2024).
42. J. O'Farrell *et al.*, *Remote Sens.* **17**, 358 (2025).
43. L. Goldberg, D. Lagomasino, N. Thomas, T. Fatoyinbo, *Glob. Change Biol.* **26**, 5844–5855 (2020).
44. V. Hagger *et al.*, *Nat. Commun.* **13**, 6373 (2022).
45. R. Bardou, D. A. Friess, T. W. Gillespie, K. C. Cavanaugh, *Glob. Ecol. Conserv.* **53**, e03022 (2024).
46. C. A. Buelow *et al.*, *Curr. Biol.* **32**, 1641–1649.e3 (2022).
47. S. S. Chand *et al.*, *Nat. Clim. Chang.* **12**, 655–661 (2022).
48. H. C. Teo *et al.*, *Nat. Sustain.* **8**, 358–362 (2025).
49. E. Monga, M. M. Mangora, J. S. Mayunga, *West. Indian Ocean J. Mar. Sci.* **17**, 1–10 (2018).
50. N. Saintilan, N. C. Wilson, K. Rogers, A. Rajkaran, K. W. Krauss, *Glob. Change Biol.* **20**, 147–157 (2014).
51. M. Jia, Z. Wang, Y. Zhang, D. Mao, C. Wang, *Int. J. Appl. Earth Obs. Geoinf.* **73**, 535–545 (2018).
52. Z. Zhang *et al.*, *Nat. Ecol. Evol.* **8**, 239–250 (2024).
53. M. P. Kumara, L. P. Jayatissa, K. W. Krauss, D. H. Phillips, M. Huxham, *Oecologia* **164**, 545–553 (2010).
54. S. Y. Lee, S. Hamilton, E. B. Barbier, J. Primavera, R. R. Lewis 3rd, *Nat. Ecol. Evol.* **3**, 870–872 (2019).
55. D. A. Friess *et al.*, *One Earth* **5**, 456–460 (2022).
56. N. Robinson *et al.*, *Nat. Clim. Chang.* **15**, 793–800 (2025).
57. P. Bunting *et al.*, Global Mangrove Watch (1996 - 2020) Version 3.0 Dataset, Zenodo (2022); https://doi.org/10.5281/zenodo.6894273.
58. M. Jia, Global 10m resolution mangrove spatial distribution dataset (2020), version V1, Science Data Bank, (2024); https://doi.org/10.57760/sciencedb.IGA.00968.
59. D. Zanaga *et al.*, ESA WorldCover 10 m 2020 v100, version v100, Zenodo (2021); https://doi.org/10.5281/zenodo.5571936.
60. C. Giri *et al.*, Global Mangrove Forests Distribution, 2000, version 1.00, NASA Socioeconomic Data and Applications Center (SEDAC) (2013); https://www.earthdata.nasa.gov/data/catalog/sedac-ciesin-sedac-lulc-mangroves-2000-1.0.
61. L. Liangyun, Z. Xiao, Time-series global 30 m wetland maps from 2000 to 2022, version v1, Zenodo (2023); https://doi.org/10.5281/zenodo.10068479.
62. Z. Zhang *et al.*, Continuous Global Mangrove Dynamics: Annual mangrove extent during 1984-2023, version v1, Zenodo (2025); https://doi.org/10.5281/zenodo.17204134.
63. Z. Zhang, Code for unexpected expansion and regrowth in Earth's mangrove forests over the past four decades, version v1, Zenodo (2026); https://doi.org/10.5281/zenodo.18161949.

ACKNOWLEDGMENTS

We thank L. Lamb-Wotton and Z. Shribman at Tulane University for assisting with PlanetScope satellite data processing. **Funding:** This work was supported by the Cochran Family Professorship in Earth and Environmental Sciences at Tulane University, endowed by Michael and Mathilda Cochran, the Louisiana Board of Regents Endowed Professorship subprogram, and the Tulane University School of Science and Engineering Resilient Habitats and Communities taskforce (to D.A.F.). **Author contributions:** Z.Z. conceived the study, developed the mangrove dynamic dataset, designed and performed the analysis, and wrote the original draft of the paper; D.A.F. contributed supervision, funding, experimental design, research questions, and draft writing. X.-P.S. contributed to the design of the validation procedure; P.B. validated our results by comparing with the ongoing Global Mangrove Watch v4.0 change dataset; V.B.A., T.T.A., and S.S.H. provided local experience in Indonesia and Myanmar for validating our findings; and all authors commented on and edited the final version of the manuscript. **Competing interests:** The authors declare that they have no competing interests. **Data, code, and materials availability:** No new materials were created in this study. All data used in this study is publicly available. Existing global-scale mangrove datasets used in this study can be accessed here: the Global Mangrove Watch v3.0 data (*57*), the High-Resolution Global Mangrove Forests in 2020 (*58*), the European Space Agency (ESA) global mangrove extent in 2020 (*59*), the Global Mangrove Forest Distribution in 2000 (*60*), and the Global Wetland Layer FCS30D (*61*). Satellite data from Landsat 4, 5, 7, 8, and 9 are freely available from the Google Earth Engine platform. PlanetScope SuperDove images used in validating our FCC data were obtained through the Planet Labs' Education and Research Program, which allowed for free-of-charge downloads of a maximum of 3000 km^2 per month. Our generated global mangrove dynamic data are available on Zenodo (*62*) and can be accessed at https://zhenzhang.users.earthengine.app/view/globalmangrovedynamic. Python code for graphics and analyses is available on GitHub at https://github.com/GIS-ZhangZhen/ContinuousGlobalMangroveDynamics and archived at Zenodo (*63*).

SUPPLEMENTARY MATERIALS

science.org/doi/10.1126/science.aec9773
Materials and Methods; Figs. S1 to S32; Tables S1 to S6; References (*64*–*97*); Data S1
Reproducibility Checklist

Submitted 10 October 2025; accepted 10 April 2026

10.1126/science.aec9773

Unexpected expansion and regrowth in Earth's mangrove forests over the past four decades

Zhen Zhang, Nicholas J. Murray, Xiao-Peng Song, Pete Bunting, Thomas A. Worthington, Lola Fatoyinbo, Dehua Mao, Mingming Jia, Virni Budi Arifanti, Toh Aung, San San Htay, and Daniel A. Friess

Science **392** (6802), . DOI: 10.1126/science.aec9773

Editor's summary

Mangrove forests are coastal habitats that serve as nurseries for economically important fisheries. Natural disturbances such as cyclones and shore erosion, together with aquaculture, palm plantation, and rice paddy expansion, have led to global declines in mangrove forest cover, spurring national and international pledges to restore it. Zhang *et al*. created a 30-meter-resolution annual dataset from satellite imagery to assess how mangrove occurrence and canopy cover have changed from 1984 to 2023. Mangroves declined globally before 2010, but have mostly recovered since then, with both forest loss and degradation (declining canopy cover) rates slowing over time. Mangroves are mostly expanding into new habitats, but also regenerating in former habitat, suggesting hope for ecosystem recovery. —Bianca Lopez